

## X-Ray Fluorescence Yields of Al, Cl, Ar, Sc, Ti, V, Mn, Fe, Co, Y, and Ag†

L. EVAN BAILEY\* AND JOHN B. SWEDLUND‡

*Nuclear Physics Department, Stanford Research Institute, Menlo Park, California*

(Received 3 January 1967)

The  $K$ -fluorescence yields of elements in the range  $13 \leq Z \leq 27$  and the  $L$ -fluorescence yields of yttrium and silver have been measured. A monochromatic x-ray beam obtained through the Ross filter difference method produced the fluorescence in foil targets and argon gas, and some of the fluorescent x rays were detected by a flow counter mounted at right angles to the primary x rays. The incident x-ray flux was determined by a measurement in the same geometry of the x-ray flux scattered by helium. The fluorescence yields and standard deviations are  $\omega_K(\text{Al}) = 0.0379 \pm 0.0023$ ,  $\omega_K(\text{Cl}) = 0.0970 \pm 0.0054$ ,  $\omega_K(\text{Ar}) = 0.119 \pm 0.007$ ,  $\omega_K(\text{Sc}) = 0.190 \pm 0.010$ ,  $\omega_K(\text{Ti}) = 0.221 \pm 0.012$ ,  $\omega_K(\text{V}) = 0.250 \pm 0.012$ ,  $\omega_K(\text{Mn}) = 0.303 \pm 0.017$ ,  $\omega_K(\text{Fe}) = 0.347 \pm 0.022$ ,  $\omega_K(\text{Co}) = 0.366 \pm 0.020$ ,  $\tilde{\omega}_L(\text{Y}) = 0.0315 \pm 0.0028$ , and  $\tilde{\omega}_L(\text{Ag}) = 0.0659 \pm 0.0037$ . The uncertainties include a 5% uncertainty in the helium-scattering cross section assumed for the data reduction. These  $K$ -fluorescence yields and the values for fluorescence yields for  $Z \geq 30$  considered best by Fink, Jopson, Mark, and Swift are fitted with the semiempirical formula  $[\omega_K/(1-\omega_K)]^n = A + BZ + CZ^2$ , using  $n = \frac{1}{4}$  and  $\frac{1}{3}$ . The best fit is given by  $[\omega_K/(1-\omega_K)]^{1/3} = -0.1019 + 0.03377Z + 1.178 \times 10^{-6}Z^2$ , with a standard deviation of 2.4%.

### INTRODUCTION

THE most recent review of fluorescence-yield measurements has been given by Fink, Jopson, Mark, and Swift.<sup>1</sup> This tabulation of fluorescence yields, as well as earlier tabulations,<sup>2,3</sup> indicates that the fluorescence-yield measurements for low-atomic-number elements show a variation between experiments that is outside the experimental uncertainty given for the individual experiments. For example, measurements of the fluorescence yield of argon can be split into a low group around 0.085<sup>4,5</sup> and a high group around 0.13.<sup>6-8</sup> A second example is the fluorescence yield of aluminum, where values of  $0.008 \pm 0.003$ ,<sup>9</sup>  $0.0381 \pm 0.0015$ ,<sup>10</sup> and  $0.045 \pm 0.002$ <sup>11</sup> are given. It is clear that there are erroneous measurements in the literature which should be discarded, but because insufficient description and data are given in some of the papers, the reader cannot choose the measurements to be discarded with complete

confidence. Thus, one is led to perform independent measurements of fluorescence yield.

In the present experiment, a monochromatic x-ray beam was used to excite the fluorescing element, and some of the fluorescent x rays were detected by a flow counter mounted at right angles to the primary x-ray beam. The primary x-ray flux was determined through helium scattering to the flow counter in the same geometrical arrangement. This method appears to generate lower backgrounds than do other methods typically used to measure the fluorescence of low-atomic-number elements. The fluorescence yield of argon was determined both by this method and by the more conventional analysis of a pulse-height spectrum obtained from a methane-argon flow counter, and thus a comparison of the two experimental methods was obtained.

The  $K$ -fluorescence yield  $\omega_K$  is defined as the probability that a  $K$  x ray is produced once a vacancy is created in the  $K$  shell. A  $K$ -shell vacancy can be filled either through a fluorescent transition in which a  $K\alpha$  or a  $K\beta$  x ray is emitted, or through a radiationless or Auger transition in which an energetic electron is emitted. If  $\Gamma_f$  is the fluorescent transition rate and  $\Gamma_a$  is the Auger transition rate, the fluorescence yield  $\omega$  is

$$\omega_K = \Gamma_f / (\Gamma_a + \Gamma_f). \quad (1)$$

The absorption of an x ray can excite any one of a number of atomic levels. In fluorescer targets that contain more than one element, this includes levels in elements other than the fluorescer element being investigated. The fraction  $f$  of the absorptions that excite the  $K$  level is normally assumed to be determinable from the jump in the absorption of the target material at the  $K$  edge of the fluorescer element. Thus

$$f = (\mu_+ - \mu_-) / \mu_+, \quad (2)$$

where  $\mu_-$  is the absorption immediately below the  $K$ -edge energy, and  $\mu_+$  is the absorption immediately

† Supported by Defense Atomic Support Agency.

\* Present address: General Atomic Division of General Dynamics Corporation, San Diego, California.

‡ Present address: University of Oregon, Eugene, Oregon.

<sup>1</sup> R. W. Fink, R. C. Jopson, H. Mark, and C. D. Swift, *Rev. Mod. Phys.* **38**, 513 (1966).

<sup>2</sup> C. D. Broyles, D. A. Thomas, and S. K. Haynes, *Phys. Rev.* **89**, 715 (1953).

<sup>3</sup> M. A. Listengarten, *Izv. Akad. Nauk SSSR, Ser. Fiz.* **24**, 1041 (1960) [English transl.: *Bull. Acad. Sci. USSR, Phys. Ser.* **24**, 1050 (1960)].

<sup>4</sup> G. R. Harrison, R. C. Crawford, and J. I. Hopkins, *Phys. Rev.* **100**, 841 (1955).

<sup>5</sup> C. Godeau, *Natl. Bur. Std. (U.S.) Tech. Note No. 91*, May, 1961.

<sup>6</sup> T. Watanabe, H. W. Schnopper, and F. N. Cirillo, *Phys. Rev.* **127**, 2055 (1962).

<sup>7</sup> Joachim Heintze, *Z. Physik* **143**, 153 (1955).

<sup>8</sup> D. L. Dexter and W. W. Beeman, *Phys. Rev.* **81**, 456 (1951).

<sup>9</sup> R. A. Rightmire, J. R. Simanton, and T. P. Kohman, *Phys. Rev.* **113**, 1069 (1959).

<sup>10</sup> A. A. Konstantinov, V. V. Perepelkin, and T. E. Sazonova, *Izv. Akad. Nauk SSSR, Ser. Fiz.* **28**, 107 (1964) [English transl.: *Bull. Acad. Sci. USSR, Phys. Ser.* **28**, 103 (1964)].

<sup>11</sup> F. Suzor and G. Charpak, *J. Phys. Radium* **20**, 462 (1959).

above the  $K$ -edge energy. If  $\mu_+$  and  $\mu_-$  include the absorption of all elements in the target, this formula is applicable to fluorescer targets containing several elements. However, we note that since the energy dependence of the x-ray absorption is not the same above and below an absorption edge, some error is introduced in the extrapolation of  $f$  determined at the absorption-edge energy to the x-ray energy exciting the fluorescer.

### EXPERIMENTAL METHOD

Figure 1 shows schematically the experimental apparatus used for fluorescence-yield measurements. X rays were generated in an x-ray tube and filtered by a  $K$ -edge absorber to produce an x-ray beam consisting principally of the  $K\alpha$  radiation characteristic of the target of the x-ray tube. Copper and chromium x-ray tubes provided  $K\alpha$  x-ray energies of 8.041 and 5.412 keV, respectively. The purity of the x-ray beam was enhanced by running the x-ray tubes at relatively low voltages of 10 to 20 kV. This minimizes the fraction of the x-ray beam due to bremsstrahlung. These x rays then passed through one member of a Ross filter pair and through a 1-mil Mylar window into an evacuated (or gas-filled) chamber. The idealized Ross filter pair consists of two filters made of elements adjacent in the periodic table, each with a thickness that makes the x-ray absorption the same for all energies except those between the  $K$  absorption edges. Experiments are performed by taking the difference between count rates obtained with each of the two filters. In this way a monochromatic x-ray flux is, in principle, produced. The purity of the Ross-filtered x-ray beam was determined by measuring the x-ray transmission of the argon-filled chamber as a function of argon pressure. The transmission-versus-pressure data fit a single exponential and indicate that the x-ray impurities in the beam were less than 1%.

The x rays were collimated in the experimental chamber and impinged on a foil containing the fluorescent element mounted at  $45^\circ$  to the x-ray beam. Fluorescent x rays were sampled by a methane-argon flow proportional counter mounted at right angles to the x-ray beam and at  $45^\circ$  to the fluorescer. The flow counter and the experimental chamber had in common a  $\frac{1}{4}$ -mil aluminized-Mylar window. The x-ray counts were pulse-height analyzed to determine their amplitude.

X rays can be scattered by the fluorescer to the detector. Since these scattered x rays have approximately the full energy of the primary x rays, they usually are separated in the pulse-height analysis. For some fluorescent elements, the scattered x-ray escape peak overlaps the main peak from fluorescent x rays. For the scattered signal to be comparable with the fluorescent signal, the crystal spacing in the fluorescer must be such that the Bragg angle is very close to  $45^\circ$  for the primary x-ray energy. For the fluorescers used in the present work, this Bragg condition was satisfied

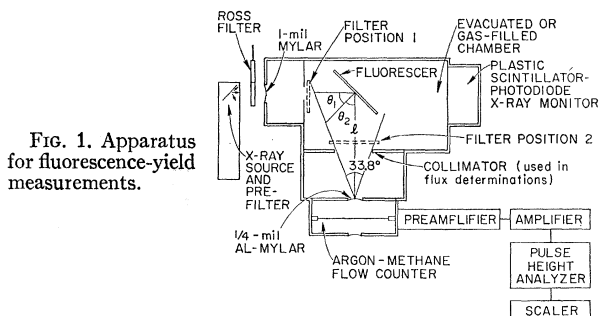


Fig. 1. Apparatus for fluorescence-yield measurements.

only in the case of chromium primary x rays on an yttrium fluorescer.

The primary x-ray flux was determined through a measurement of the x-ray flux scattered by helium using published values for the coherent- and incoherent-scattering cross section.<sup>12-14</sup> The fluorescer is removed from the x-ray beam and the chamber is filled with helium to a pressure of about 1 atm, the exact pressure being measured with a mercury manometer and the gas temperature with a thermometer inside the chamber. The advantages of this technique are (1) some of the geometrical factors cancel between the fluorescence-yield and flux measurement, (2) the x-ray flux can be measured concurrently with the fluorescence yield, and (3) scattering is the most straightforward and accurate method of reducing the flux by the large amounts necessary to count individual x rays. The disadvantages of the method are (1) that the fluorescence-yield measurements rely on an accurate knowledge of the helium-scattering cross section, and (2) that the polarization of the primary x-ray flux must be determined. An error in the helium-scattering cross section or the degree of polarization introduces the same fractional error into all of the fluorescence-yield measurements. X rays scattered at  $90^\circ$  are plane-polarized with the electric vector perpendicular to the scattering plane. Since most of the flux used in the measurement consists of characteristic x rays, it is expected that the primary flux in the band selected by the Ross filter is only very slightly polarized. The polarization of the Ross-filtered x-ray beam was determined experimentally to be less than 1% for both the chromium and copper x-ray tubes.

Two flow counters were used whose linear dimensions differed by a factor of 3. The smaller counter was a cylinder with an i.d. of 0.875 in. and a length of 2.625 in. The aluminized-Mylar entrance and exit windows to the counter were parallel and 0.937 in. apart. (The front window of the counter bowed when the chamber was evacuated to give an average thickness of 0.9675 in.) The central wire of the counter was 0.5-mil tungsten.

<sup>12</sup> *International Tables for X-ray Crystallography* (The Kynoch Press, Birmingham, England, 1962), Vol. III.

<sup>13</sup> A. H. Compton and S. K. Allison, *X-Rays in Theory and Experiment* (D. Van Nostrand Company, Inc., New York, 1935).

<sup>14</sup> R. J. Stinner, W. H. McMaster, and N. K. Del Grande, University of California Radiation Laboratory Report No. UCRL-14403, 1965 (unpublished).

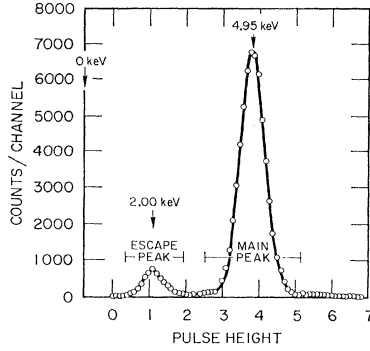


FIG. 2. Pulse-height spectrum in small flow counter from vanadium  $K$  x rays.

A 90% argon-10% methane mixture was used as the counter gas. The x-ray counts were pulse-height analyzed, producing two different characteristic pulse-height spectra as shown in Figs. 2 and 3, depending on x-ray energy. For x rays more energetic than 3.203 keV, a two-peak spectrum was obtained (Fig. 2) with the main peak corresponding to the full energy of the absorbed x ray, and the smaller or escape peak corresponding to the energy of the absorbed x ray less the energy of the argon fluorescent x ray that escaped from the counter. For x rays less energetic than the  $K$  edge of argon, a single peak was obtained (Fig. 3) corresponding to the energy of the absorbed x ray. The high-energy peak in Fig. 3 is due to scattered x rays and is easily separated from the fluorescent energy peak. The procedure was to run a pulse-height analysis on the fluorescent or helium-scattered x rays; then channel limits were set to count all x rays from below the escape peak to above the main peak. If the pulse-height analysis in the fluorescent part of the measurement indicated scattered x rays were present in the integrated signal, the fraction of the signal due to scattered x rays was estimated and the observed count rate corrected. In the more typical pulse-height spectra shown in Figs. 2 and 3, some counts appear both above and below the main peak. That these counts come from the fluorescer is demonstrated by removing the fluorescer from the primary beam and observing that the count rate goes to essentially zero. If these counts were assumed to be due to background and were extrapolated through

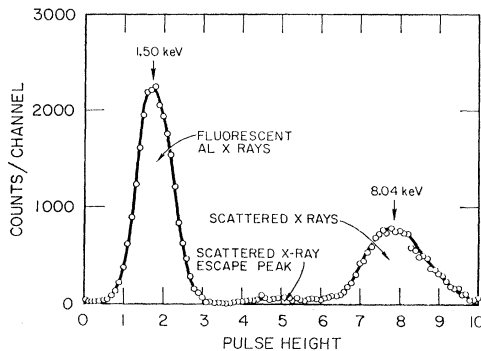


FIG. 3. Pulse-height spectrum from Al  $K$  x rays.

the limits of integration, the net number of counts would change by between 1 and 2%. This change would occur in both the fluorescence- and helium-scattered counts. Thus, we conclude that the uncertainty due to background is no more than 1%. These counts no doubt result from (1) x rays of the wrong energy, i.e., scattered rather than fluorescent x rays, being detected, (2) x rays absorbed in the counter gas whose resulting electrons are partially stopped in the counter walls, and (3) x rays absorbed in the counter walls whose resulting electrons are partially stopped in the counter gas.

Except for argon gas, the fluorescence-yield measurements were made using thin foils. Elemental foils of Al, Sc, Ti, V, Fe, Co, Y, and Ag were used. Cl was used in the form of Saran ( $H_2CCl_2$ )<sub>n</sub>. The Mn foils were an alloy containing approximately 96.7% Mn, 2% Cu, 1% Ni, and 0.3% Fe; pure Mn metal could not be rolled into thin foils.

The count rate due to fluorescent x rays from a foil target  $N_f$  as the result of a primary x-ray flux  $N_0$  is

$$N_f = \omega f N_0 \frac{A_c \{1 - \exp(-\lambda_f / \cos \theta_1 - \lambda_{fK} / \cos \theta_2)\}}{4\pi l^2 [1 + (\lambda_{fK} \cos \theta_1 / \lambda_f \cos \theta_2)]} \times [\exp(-\lambda_w K)] \{1 - \exp(-\lambda_c K)\}, \quad (3)$$

where  $\omega$  is  $\omega_K$  or  $\bar{\omega}_L$ ,  $A_c$  is the counter-aperture area,  $l$  is the fluorescer-counter distance,  $\theta_1$  and  $\theta_2$  are the angle of the primary and fluorescent x ray with respect to the foil normal, respectively, and  $\lambda$  is the x-ray absorption of the various components of the experimental system. Subscripts are assigned to indicate both the component in the system (subscript  $f$  for fluorescer,  $w$  for counter window, and  $c$  for counter gas) and the x-ray energy (no subscript for the primary x-ray energy and subscript  $K$  for the fluorescent x-ray energy).

With the experimental chamber filled with helium to a density  $\rho_{He}$ , the scattered x-ray flux  $N_s$  is

$$N_s = N_0 \frac{N_A}{A} \exp(-\lambda_w) [1 - \exp(-\lambda_c)] \int_{-x_0}^{x_0} \frac{d\sigma}{d\Omega}(\theta) \times \exp(-\lambda_{He}) \rho_{He} \Omega dx, \quad (4)$$

where  $N_A$  is Avogadro's number,  $A$  is the atomic weight of the scattering gas,  $x$  is distance measured in the primary flux (only elements of gas between  $-x_0$  and  $+x_0$  scatter to the counter),  $\Omega$  is the solid angle subtended by the flow counter, and  $(d\sigma/d\Omega)(\theta)$  is the cross section per atom per steradian for scattering x rays at angle  $\theta$ . For a counter aperture of zero thickness,  $\Omega = A_c \sin \theta / (l^2 + x^2)$ . However, the counter aperture is of finite thickness, thus reducing the aperture area slightly, and this effect is included in our calculations. The terms  $\lambda_w$  and  $\lambda_c$  are evaluated at the average energy of the scattered x rays which energy is slightly

lower than the primary x-ray energy because of the loss of energy in incoherent or Compton scattering. Values of  $(d\sigma/d\Omega)(\theta)$  can be determined from theoretical data on coherent and incoherent scattering given in Refs. 12 and 13. These calculations have been performed by Stinner *et al.*<sup>14</sup>; they determine  $(d\sigma/d\Omega)(90^\circ)$  for helium to be  $9.90 \times 10^{-26}$  cm<sup>2</sup>/sr atom at 5.412 keV and  $8.40 \times 10^{-26}$  cm<sup>2</sup>/sr atom at 8.041 keV. Using these values the fluorescence-yield measured with chromium x rays is 5% higher than when measured with copper x rays. The measurements of Wollan<sup>15</sup> indicate that the scattering of x rays by helium at low energies (or small angles) is less than predicted theoretically. To bring our measurements with the two x-ray sources into accord we used  $(d\sigma/d\Omega)(90^\circ) = 9.42 \times 10^{-26}$  cm<sup>2</sup>/sr atom at 5.412 keV and  $(d\sigma/d\Omega)(90^\circ) = 8.40 \times 10^{-26}$  cm<sup>2</sup>/sr atom at 8.041 keV. The angle dependence of scattering in the  $\pm 17^\circ$  angle accepted by the counter is well approximated by

$$\frac{d\sigma}{d\Omega}(\theta) = \left[ \frac{d\sigma}{d\Omega}(90^\circ) + a(90^\circ - \theta) \right] (1 + \cos^2\theta).$$

Since the term  $a(90^\circ - \theta)$  is symmetrical about  $90^\circ$ , it does not contribute to the integral in Eq. (4).

With the experimental chamber filled with argon, the count rate due to argon fluorescence is

$$N_f = \omega_{Kf} N_0 \exp(-\lambda_f - \lambda_{wK}) [1 - \exp(-\lambda_{cK})] \times \int_{-x_0}^{x_0} \frac{\Omega}{4\pi} \mu_f \rho \exp[-\mu_f \rho x - (x^2 + l^2)^{1/2} \mu_{fK} \rho] dx, \quad (5)$$

where  $\exp(-\lambda_f)$  is the attenuation of the argon measured to the center of the experimental chamber (at  $x=0$ ),  $\mu_f$  is the mass absorption of argon primary x rays,  $\mu_{fK}$  is the x-ray absorption of argon for fluorescent x rays, and  $\rho$  is argon density.

The x-ray absorption of the various components was measured using the Ross filter difference technique for both primary and fluorescent x rays. A second fluorescer of approximately the same thickness as the experimental fluorescer was inserted in the fluorescer position.

The transmission of the experimental fluorescer to the primary x rays [ $\exp(-\lambda_f)$ ] was then determined by placing it in and out of filter position 1 (see Fig. 1) and counting x rays from the second fluorescer. Similarly, the transmission of the experimental foil and the counter window to fluorescent x rays [ $\exp(-\lambda_{fK})$  and  $\exp(-\lambda_{wK})$ ] are found by placing them in and out of filter position 2. The transmission of the counter window to primary x rays [ $\exp(-\lambda_w)$ ] is determined with the counter window in filter position 2 using a helium-gas scatterer. The transmission of methane-argon to primary x rays [ $\exp(-\lambda_c)$ ] is determined by filling the experimental chamber with counter gas and measuring the transmission as a function of pressure with the plastic scintillator—photodiode x-ray monitor.

The advantage of measuring transmission with these techniques is that transmissions are determined for the actual x-ray composition of the primary and fluorescent x-ray fluxes. For example, continuum x rays in the energy band selected by the Ross filter could change the average energy of the primary x-ray fluxes from the values given above. Similarly, one avoids the requirement of estimating the relative amounts of  $K\alpha$  and  $K\beta$  x rays (or of the various  $L$  lines) in the fluorescent flux from each fluorescer and then computing the average energy of the fluorescent x rays. Experimental measurements of absorption were not made for helium, for argon in the argon fluorescence experiment, or for the methane-argon counter gas at the fluorescent x-ray energy. Instead, published mass-absorption coefficients for the elements involved were used. Since the x-ray absorption in helium is small, the error arising from the use of the wrong absorption in helium is negligible. The uncertainty in the fluorescence yield stemming from uncertainty in counter absorption is minimized by using the larger of the two flow counters.

## RESULTS

Two or more runs were made for each fluorescer element using the x-ray fluxes that could excite the fluorescer. Experimental data obtained in typical runs are given in Table I. Each run yielded a value of  $\omega f$ .

TABLE I. Experimental data from typical runs on each fluorescer.

Element	Foil thickness (mg/cm <sup>2</sup> )	Primary energy (keV)	Counter thickness (inches)	Net fluorescent x-ray flux (counts/sec)	Net He scattered flux (counts/sec)	$\exp(-\lambda_{fK})$	$\exp(-\lambda_f)$	$\exp(-\lambda_{wK})$	$\omega_{Kf}$ or $\bar{\omega}_{Lf}$ (this run)	Average $\omega_{Kf}$ or $\bar{\omega}_{Lf}$
Al	1.93	5.41	0.9675	2578	100.88	0.4593	0.7396	0.4434	0.0342	0.0352
Al	1.53	8.04	0.9675	570.9	30.59	0.5198	0.9236	0.4434	0.0354	0.0352
Y	0.85	8.04	2.718	769	64.36	0.4716	0.8934	0.654	0.0244	0.0246
Y	0.79	5.41	2.718	2648	131.1	0.5024	0.747	0.654	0.0257	0.0246
Cl (Saran)	2.94	8.04	2.718	1357	13.099	0.566	0.8025	0.8377	0.0878	0.0862
Ag	1.13	5.41	2.718	2012	21.95	0.5341	0.4742	0.8990	0.0531	0.0511
Ag	1.13	8.04	2.718	826.6	13.195	0.5341	0.7734	0.8990	0.0496	0.0511
Sc	2.21	8.04	2.718	3795	7.680	0.7561	0.6598	0.9587	0.1692	0.1697
Ti	2.49	5.41	2.718	4801	6.254	0.7817	0.2461	0.9618	0.193	0.195
V	3.89	8.04	2.718	4448	4.585	0.7278	0.4653	0.9764	0.2228	0.2224
Mn (Mn alloy)	5.3	8.04	2.718	5461	3.733	0.6475	0.2193	0.9833	0.2670	0.2683
Fe	0.5	8.04	2.718	4670	8.710	0.9591	0.8338	0.987	0.3385	0.3049
Co	8.6	8.04	2.718	4974	2.672	0.5937	0.0462	0.988	0.3262	0.3274

<sup>15</sup> E. O. Wollan, Phys. Rev. **37**, 862 (1931).

TABLE II. Fluorescence yields and fluorescence-yield standard deviations,  $\Delta\omega$ .

Z	Element	$\omega_K f$	$f$	$\omega_K$	$\Delta\omega^a$	$\Delta\omega^b$
K-fluorescers						
13	Al	0.0352	0.930	0.0379	0.0013	0.0023
17	Cl (Saran)	0.0862	0.889	0.0970	0.0024	0.0054
18	Ar	0.1062	0.894	0.119	0.0034	0.007
21	Sc	0.1697	0.895	0.190	0.005	0.010
22	Ti	0.195	0.883	0.221	0.005	0.012
23	V	0.2224	0.888	0.250	0.006	0.012
25	Mn	0.2683	0.886	0.303	0.008	0.017
26	Fe	0.3049	0.878	0.347	0.014	0.022
27	Co	0.3274	0.895	0.366	0.008	0.020
L-fluorescers						
		$\bar{\omega}_L f$	$f$	$\bar{\omega}_L$	$\Delta\omega^a$	$\Delta\omega^b$
39	Y	0.0246	0.782	0.0315	0.0024	0.0028
47	Ag	0.0511	0.775	0.0659	0.0017	0.0037

<sup>a</sup> Assuming a 1% uncertainty in  $d\sigma/d\Omega$ .

<sup>b</sup> Assuming a 5% uncertainty in  $d\sigma/d\Omega$ .

These  $\omega f$  values were averaged separately for each x-ray source, and the final  $\omega f$  was determined by averaging the results from the two x-ray sources. Table II gives  $\omega f$  determined from the several runs, the assumed value for  $f$ , the resultant value for the fluorescence yield, and the estimate of the uncertainty (standard deviation) in the fluorescence yield. Table III lists the various factors that enter into the calculation of  $\omega$  and the estimate of the uncertainty in these factors. We are unable to estimate the uncertainty in the helium-scattering cross section because this cross

section is determined theoretically rather than experimentally. Since helium is a relatively simple atom, one would expect that the scattering could be computed accurately. We would expect the theoretical helium-scattering cross section to be more accurate at the higher of the two primary x-ray energies and, in fact, we have normalized the chromium x-ray measurements to the copper x-ray measurements. The uncertainty in  $\omega$  due to each of the listed factors was computed assuming both 1 and 5% for the uncertainty in  $d\sigma/d\Omega$ , and the total uncertainty was found using the sum of the square rule. Since a good part of the uncertainty is due to systematic errors, the repetition of measurements does not significantly increase the accuracy of the final result. Therefore, the uncertainty assigned to the fluorescence yield is that calculated for a single measurement. For a given fluorescer, both the computed uncertainty and observed spread in  $\omega f$  were different for the two primary x-ray fluxes with the smaller uncertainty obtained for chromium x rays. In most cases, we have assigned the smaller of the two calculated uncertainties to the fluorescence yield. In the case of yttrium, the yttrium fluorescer scattered an appreciable number of chromium x rays to the counter. A comparison of the results using the two x-ray sources indicated that the correction for scattering was properly determined and made; however, we have conservatively assigned the copper x-ray source uncertainty to this measurement.

TABLE III. Factors contributing to uncertainty in  $\omega_K$  or  $\bar{\omega}_L$  computed using Eqs. (2)-(5).

Term	Uncertainty (standard deviation)	Comment
$f$	1%	Obtained from literature.
$d\sigma/d\Omega(\theta)$	1%, 5%	Must guess this uncertainty. We use both values in computation of $\Delta\omega$ .
$N_f$	1%	Counting statistics, uncertainty in correction due to scattered x rays.
$N_s$	1%	Counting statistics.
$\exp(-\lambda_f)$	1% <sup>a</sup>	Counting statistics, nonuniformity of foils. <sup>b</sup>
$\exp(-\lambda_{fK})$	1% <sup>a</sup>	Counting statistics, nonuniformity of foils. <sup>b</sup>
$\exp(-\lambda_w), \exp(-\lambda_{wK})$	1% <sup>a</sup>	Counting statistics.
$\lambda_c, \lambda_{cK}$	2%	Deviations from 90% argon-10% methane, pressure and temperature variations, uncertainty in x-ray mass absorption tables, variations in counter thickness due to window bowing.
$\theta_1, \theta_2$	$\Delta\theta_1 = \Delta\theta_2 = \frac{1}{2}^\circ$	Misorientation of fluorescer.
$\rho_{He}$	0.36%	Pressure and temperature uncertainties.
Physical dimensions $A_c, l, x_0$	Negligible	
Physical constants $N_A, A$	Negligible	

<sup>a</sup> Typical uncertainty. Value computed from counting statistics was used in calculation of uncertainty in  $\omega$ .

<sup>b</sup> Nonuniformity of foils is important only when  $\exp(-\lambda)$  is small.

Yields of  $L$  fluorescence were measured for yttrium ( $Z=39$ ) and silver ( $Z=47$ ). The experimental and data-analysis techniques were essentially the same as for  $K$ -fluorescence-yield measurements. The fraction of x-ray absorptions that create vacancies in the  $L$  levels  $f_L$ , was determined by extrapolating the x-ray absorption at energies above the  $L_3$  edge to the  $L_1$  edge, and then using Eq. (2) to determine  $f_L$ . Silver  $L$  x rays fall both above and below the  $K$  edge of argon. Most of the silver  $L$  x rays ( $\sim 94\%$ ) are below the  $K$  edge of argon, and an energy of 3.02 keV was used in computing the absorption of x rays in the counter.

#### A CONVENTIONAL DETERMINATION OF THE FLUORESCENCE YIELD OF ARGON

The fluorescence yield of argon can be determined from an analysis of the pulse-height spectrum produced by the absorption of x rays in a flow counter; Fig. 2, is the spectrum from the absorption of vanadium  $K$  x rays in the smaller of the two flow counters. The counts  $N_a$  in the main peak are the result of x-ray absorptions followed by Auger transitions or  $K$  fluorescences in which the fluorescent x ray is absorbed in the counter gas. The counts  $N_e$  in the escape peak are the result of  $K$  x rays escaping from the counter gas. If  $p$  is the probability that a fluorescent x ray escapes, then

$$\omega_K f = (1/p)N_e / (N_e + N_a).$$

The geometry of the flow counter is shown in Fig. 4. The counter is approximated as a cylinder of diameter  $2r_0$  and height  $2h_0$ . X rays enter the counter in a well-defined beam centered at  $h_0$  and on a diameter of the counter. Let  $\mu$  be the absorption of the methane-argon mixture for the incident x rays,  $\mu_K$  be the absorption for the fluorescent argon x rays, and  $\rho$  the density of the gas mixture. Then, the probability that a fluorescent x ray escapes when the incident x ray is in the center of the beam is

$$p = \frac{\frac{1}{4\pi} \int_0^{2r_0} e^{-\mu\rho x} \int_0^{2\pi} \int_0^\pi e^{-\mu_K\rho y(x,\varphi,\theta)} \sin\theta d\theta d\varphi dx}{\int_0^{2r_0} e^{-\mu\rho x} dx}, \quad (6)$$

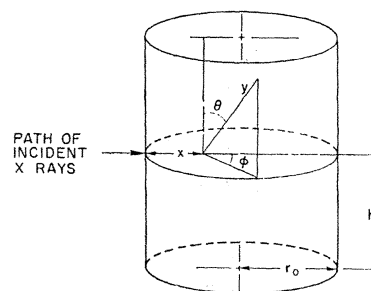
where  $y(x,\varphi,\theta)$  is the path length of an escaping x ray generated at  $x$  and emitted in the direction  $\varphi$ ,  $\theta$ . This path length is

$$y = \frac{(r_0 - x) \cos\varphi + [r_0^2 - (r_0 - x)^2 \sin^2\varphi]^{1/2}}{\sin\theta}$$

for

$$\{(r_0 - x) \cos\varphi + [r_0^2 - (r_0 - x)^2 \sin^2\varphi]^{1/2}\} > h_0 \tan\theta$$

FIG. 4. Geometry of flow counter.



and  $y = h_0 / \cos\theta$  otherwise.<sup>16</sup> The value of  $p$  was determined through numerical integration using a computer. The model of the counter used in the calculation of  $p$  is simplified from the actual counter. Effects which were neglected include (1) shadowing by the central wire of the counter, (2) the finite size of the x-ray beam entering the counter, and (3) the planar rather than cylindrical geometry at the entrance (and exit) window of the counter. We assert without proof that these simplifications result in a small error in the calculated  $p$ .

The results of the pulse-height analysis to determine the fluorescence yield of argon are given in Table IV. It can be seen that the two methods of measuring the fluorescence yield of argon are in good agreement.

The largest uncertainty in this measurement is the determination of the number of background counts, especially in the escape peak. The limits of integration were chosen as shown in Fig. 2. It was assumed that there were no background counts in either the main peak or the escape peak, or equivalently that the fraction of counts in each peak due to background is the same. By attributing the count rates observed on both sides of each peak to background and interpolating these count rates through the peaks, one would deduce that 10% of the signal in the escape peak is background and that 5% of the signal in the main peak is background. This would change the fluorescence yield by 5%. The probability  $p$  is very insensitive to the absorption coefficient for the incident x rays. A 5% uncertainty in the absorption of the fluorescent x rays leads to a 1.5% change in  $p$ . Using a 1% uncertainty in  $f$ , we calculate the uncertainty in  $\omega$  to be 5.3%.

TABLE IV. The fluorescence yield of argon from pulse-height spectra.

Fluorescer	$N_f$	$N_a$	$p$	$\omega_K f$	$f$	$\omega_K$
Sc	15630	185209	0.7195	0.1088		
V (Run 1)	12327	144888	0.7158	0.1095		
V (Run 2) (Fig. 3)	5037	59504	0.7158	0.1090		
Average				0.1091	0.894	0.122

<sup>16</sup> These equations for  $y$  are correct for  $0 \leq x \leq r_0$ . In the region  $r_0 \leq x \leq 2r_0$ , they are correct if  $\varphi$  is redefined as  $\varphi + \pi$ . Since  $\varphi$  is integrated from 0 to  $2\pi$ , the equations yield the correct result as is.

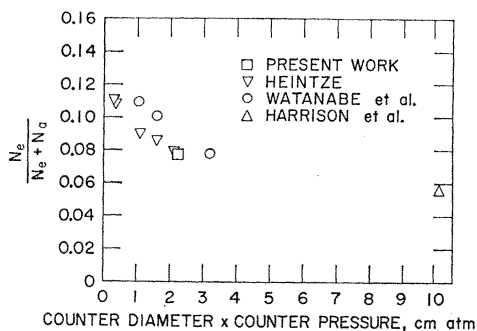


Fig. 5. The ratio of counts in the escape peak to total counts as a function of (counter pressure)  $\times$  (counter diameter) for argon proportional counters. This analysis suggests that Watanabe *et al.* used a slightly different criteria in correcting for background counts than did Heintze or the present authors. It also suggests that Harrison *et al.* did not properly correct for the absorption of fluorescent x rays in the counter gas.

Thus the fluorescence yield of argon determined through an analysis of a pulse-height spectrum is

$$\omega_K = 0.122 \pm 0.0065.$$

The analysis of a pulse-height spectrum to determine the fluorescence yield of argon has been used by Harrison *et al.*,<sup>4</sup> Heintze,<sup>7</sup> and Watanabe *et al.*,<sup>6</sup> who obtained the values  $0.081 \pm 0.006$ ,  $0.129 \pm 0.01$ , and  $0.14 \pm 0.014$ , respectively. Our measurement is in reasonable agreement with the last two and is in disagreement with the first measurement. Numerical data are available in the Heintze and Watanabe papers that allow one to investigate the cause of the differences in the several measurements. To this end we plot in Fig. 5 the quantity  $N_e/(N_e + N_a)$  versus (counter pressure)  $\times$  (counter diameter). The value attributed to Harrison *et al.* was determined from a pulse-height spectrum presented in that paper. It can be seen that Harrison *et al.* used a much larger counter and that their datum point does not fall low with respect to the extension of the other data points. We conclude that Harrison *et al.* did not make the proper correction for captured fluorescent x rays, and therefore the fluorescence yield given in that paper is not a valid measurement. In Fig. 5, our measurement appears to coincide with the Heintze measurement; yet our fluorescence yield differs from his by 5.5%. The reason for the difference is that he used a higher value for the absorption of fluorescent x rays in the counter gas in his calculation of  $p$ , as if his experiment were run near 0°C, rather than at our more comfortable 25°C. Heintze derived an analytic formula for  $p$  which agrees with the results obtained through our computer integration of Eq. (6). The values for  $N_e/(N_e + N_a)$  of Watanabe *et al.* are high with respect to the Heintze values and our value, as if slightly different criteria were used in assigning counts to the two peaks and eliminating background.<sup>17</sup>

<sup>17</sup> Rather than calculate  $p$ , Watanabe measured  $N_e/(N_e + N_a)$  versus counter pressure and extrapolated to zero counter pressure.

## DISCUSSION

Attempts have been made to fit  $K$ -fluorescence yields to the semiempirical formula

$$[\omega_K/(1-\omega_K)]^{1/4} = A + BZ + CZ^3 = B(Z + A/B) + CZ^3.$$

Burhop<sup>18</sup> gives this formula the following physical basis: The magnitude of the fluorescence yield is determined by competition between the fluorescence effect and the Auger effect. Through quantum-mechanical calculations it is argued that the Auger transition rate is almost independent of atomic number, and that the fluorescence transition rate increases approximately with the fourth power of atomic number. Thus

$$\omega_K = (BZ)^4/[1 + (BZ)^4],$$

where  $B$  is a constant. Performing the algebra, we find

$$[\omega_K/(1-\omega_K)]^{1/4} = BZ.$$

The terms  $A$  and  $CZ^3$  are included in the semiempirical formula and are attributed to screening and a relativistic correction, respectively. If  $A$  is due to screening, then  $A$  should be negative.

We have determined new values for  $A$ ,  $B$ , and  $C$  using our data for  $13 \leq Z \leq 27$  and the judgment of Fink *et al.*<sup>1</sup> of the best value for the fluorescence yields for  $Z \geq 30$  as given in Table V. The result is

$$[\omega_K/(1-\omega_K)]^{1/4} = 0.0408 + 0.0315Z - 0.828 \times 10^{-6}Z^3. \quad (7)$$

The constants were determined using the method of least squares in which the function

$$\chi^2 = \sum \left[ - (1-\omega_K) + \frac{A + BZ + CZ^3}{[\omega_K/(1-\omega_K)]^{1/4} [1/(1-\omega_K)]} \right]^2$$

TABLE V. Fluorescence yields measured and calculated from semiempirical formulas.

$Z$	$\omega_K$ from present measurements and Ref. 1	$\omega_K$ calculated from $\frac{1}{4}$ power law, Eq. (7)	$\omega_K$ calculated from $\frac{1}{3}$ power law, Eq. (8)
13	0.0379	0.0389	0.0377
17	0.097	0.0968	0.0984
18	0.119	0.117	0.119
21	0.190	0.189	0.191
22	0.221	0.216	0.218
23	0.250	0.245	0.247
25	0.303	0.307	0.306
26	0.347	0.338	0.336
27	0.366	0.370	0.366
30	0.433	0.463	0.456
32	0.500	0.521	0.513
34	0.570	0.576	0.566
36	0.630	0.625	0.615
40	0.730	0.708	0.699
50	0.863	0.840	0.839
60	0.913	0.904	0.912
70	0.943	0.937	0.950
80	0.96	0.954	0.970
90	0.966	0.964	0.982

<sup>18</sup> E. H. S. Burhop, *The Auger Effect* (Cambridge University Press, London, 1952).

was minimized with respect to  $A$ ,  $B$ , and  $C$  to give three simultaneous equations in  $A$ ,  $B$ , and  $C$ . This particular function was chosen because it weights to the same degree the percentage uncertainty in each value of  $\omega_K$ , i.e., it assumes that  $\Delta\omega/\omega_K = \text{constant}$ . The data chosen for the least-squares analysis weight our data and the data of Fink *et al.* about equally in the region where the two curves join. The average percentage difference (standard deviation) between the fluorescence yield calculated from this formula and the fluorescence yield used as input for the calculation is 2.7%. The largest percentage difference of 7% occurs in the vicinity of  $Z=30$  and is the consequence of our data not smoothly joining the fluorescence-yield curve of Fink *et al.* The Fink *et al.* curve is low with respect to the extrapolation of our data in the  $Z$  region of 27 to 40. It should be noted that the first term of the semiempirical formula has the wrong sign to be interpreted as a screening term.

The theoretical fluorescence yields of Callan<sup>19</sup> when fit to the semiempirical formula using the method of least squares also give a positive screening term. A consideration of the manner in which Callan determines  $\omega_K$  indicates that the uncertainty in each calculated  $\omega_K$  is proportional to  $\omega_K(1-\omega_K)$ . Thus the function to be minimized is

$$\chi^2 = \sum \left( -1 + \frac{A + BZ + CZ^3}{[\omega_K/(1-\omega_K)]^{1/4}} \right)^2,$$

with the result

$$[\omega_K/(1-\omega_K)]^{1/4} = 0.0376 + 0.0321Z - 0.875 \times 10^{-6}Z^3.$$

An examination of the Auger radiation widths used by Callan indicates that the Auger transition rate is directly proportional to  $Z$  (rather than independent of  $Z$ ) and that the fluorescence transition rate is proportional to  $Z^4$ . This contradicts the assumption made in the derivation of the above semiempirical formula, and in fact leads to a new formula.

$$[\omega_K/(1-\omega_K)]^{1/3} = A + BZ + CZ^3,$$

where the  $\frac{1}{3}$  power replaces the  $\frac{1}{4}$  power. A determination of the constants for our data and the data of Fink *et al.* as described above yields

$$[\omega_K/(1-\omega_K)]^{1/3} = -0.1019 + 0.03377Z + 1.177 \times 10^{-6}Z^3. \quad (8)$$

The average percentage difference was 2.4%, again with the largest difference of  $\sim 5.3\%$  at  $Z=30$ . We now

<sup>19</sup> E. J. Callan, (unpublished); Bull. Am. Phys. Soc. 7, 416 (1962).

have a negative screening term with a screening charge  $A/B$  of  $\sim 3$ .

The input  $\omega_K$ 's and the calculated  $\omega_K$ 's from both the  $\frac{1}{4}$  law and  $\frac{1}{3}$  law are given in Table V.

The interpretation and comparison of  $L$ -fluorescence-yield measurements is more complicated than for  $K$ -fluorescence measurements. The absorption of an x ray can excite any one of the three  $L$  levels; in the present experiment the relative excitation rate is assumed to be determinable from the jump in absorption coefficients at the three  $L$  edges. In addition, the  $L_1$  and  $L_2$  levels can decay through fluorescent transitions, Auger transitions, or Coster-Kronig transitions. Coster-Kronig transitions are radiationless transitions that move a vacancy in one  $L$  shell to another ( $L_1 \rightarrow L_3$ ,  $L_1 \rightarrow L_2$ , or  $L_2 \rightarrow L_3$ ). These secondary  $L$  levels can in turn decay through the two or three processes. Only experiments in which primary x rays excite the  $L$  level can be compared directly with this experiment; other excitation methods will produce different ratios of primary vacancies in the  $L$  shells.

Suzor and Charpak<sup>20</sup> have measured the fluorescence yield of Al, and Bertrand, Charpak, and Suzor<sup>20</sup> have measured the fluorescent yield of Cl, Ni, and Ag ( $L$  yield). They obtained a higher yield for Al (0.045) and a lower yield for Cl (0.093) and Ag (0.047) than did we in the present experiment. In their experiment radioactive iron which generates Mn  $K$  x rays was deposited on foils of the fluorescing element. These foils also served as the window to the proportional counter. Corrections were made for geometry and the absorption of both primary and fluorescent x rays in the foil and in the counter, and the fluorescence yield was determined from the relative number of primary and fluorescent x-ray counts. As the pulse-height spectra in those papers show, this method requires an appreciable correction for primary x rays that produce counts in the fluorescent x-ray peak. We suggest that the differences between their results and our results are due to this effect, which, except for a few scattered primary x rays, is avoided in our measurement.

Konstantinov *et al.*<sup>10</sup> using the same experimental technique as Suzor and Charpak, have measured a fluorescence yield for aluminum of  $0.0381 \pm 0.0015$  which is in good agreement with our measurement.<sup>21</sup>

<sup>20</sup> F. Bertrand, G. Charpak, and F. Suzor, J. Phys. Radium 20, 956 (1959).

<sup>21</sup> Note added in proof: A. Mukerji [Bull. Am. Phys. Soc. 12, 69 (1967); Nucl. Phys. (to be published)] using radioactive sources has measured the following fluorescence yields:  $\omega_K(\text{V}) = 0.222 \pm 0.018$ ,  $\omega_K(\text{Fe}) = 0.322 \pm 0.029$ , and  $\omega_K(\text{Cu}) = 0.445 \pm 0.036$ . The corresponding yields calculated with Eq. (8) for V, Fe, and Cu are 0.247, 0.336, and 0.427, respectively.